https://doi.org/10.30799/jnst.S203.26110303 J. Nanosci. Tech. - Volume 11 Issue 3 (2026) 1086–1089

Share Your Innovations through JACS Directory

Journal of Nanoscience and Technology

Visit Journal at https://www.jacsdirectory.com/jnst

ISSN: 2455-0191

Synthesis and Characterization of TiO_2 Nanoparticles for Gas Sensing Applications

Purva B. Patil*, Gokul V. Suryawanshi, Tulshidas S. Savale

Department of Chemistry, M.G.V's M.S.G. Arts, Science and Commerce College, Malegaon Camp, Malegaon, Nashik – 423 105, Maharashtra, India.

ARTICLEDETAILS

Article history:
Received 24 February 2026
Accepted 11 March 2026
Available online 15 April 2026

Keywords:
TiO_2
Hydrothermal
Gas Sensor
Nanocrystal

ABSTRACT

Nanostructured titanium dioxide (TiO_2) has attracted significant attention due to its excellent physicochemical properties and promising performance in gas-sensing applications. In this study, alkoxide-derived TiO_2 gel was subjected to hydrothermal treatment at 150 °C for 3 h in diluted nitric acid solutions of pH 2 and pH 3 in order to obtain nanocrystalline TiO_2 with enhanced thermal stability. The influence of hydrothermal conditions on phase stability, crystallite growth, morphology, and gas-sensing behavior was systematically investigated. Structural evolution and phase composition of TiO_2 powders were analyzed using X-ray diffraction (XRD), while the surface morphology and particle size were examined using field-emission scanning electron microscopy (FE-SEM). The results demonstrate that hydrothermal treatment significantly improves the thermal stability of TiO_2 through two primary mechanisms: suppression of crystallite growth during calcination and an increase in the anatase-to-rutile phase transformation temperature. However, the extent of stabilization strongly depended on the pH of the nitric acid solution. Untreated TiO_2 powders exhibited predominant rutile phase formation when calcined at 700 °C. In contrast, TiO_2 powders hydrothermally treated at pH 3 retained a high fraction of the anatase phase even after calcination at elevated temperatures. After calcination at 600 and 800 °C, these samples consisted of fine anatase nanospheres with average particle sizes of approximately 13 nm and 34 nm, respectively. Correspondingly, the anatase crystallite sizes were estimated to be around 11 nm and 26 nm at 600 and 800 °C, confirming a pronounced inhibition of crystallite growth due to hydrothermal processing. Despite the reduced crystallite size, the anatase-to-rutile transformation was not completely suppressed. For the TiO_2 sample hydrothermally treated at pH 3, the rutile phase fraction increased progressively with calcination temperature, reaching approximately 9%, 22%, and 67% at 600, 700, and 800 °C, respectively. These observations indicate that crystallite size alone does not exclusively govern the phase transformation behavior of TiO_2, and that other factors such as defect chemistry, surface energy, and acid-induced structural modifications also play important roles. Gas-sensing properties were evaluated using thick-film sensors fabricated from the prepared TiO_2 powders. Although the hydrothermally treated powders particularly those processed at pH 3 exhibited slightly higher sensitivity, the overall sensor response toward diluted carbon monoxide (CO) in air at operating temperatures between 400 and 550 °C showed only minor variation among the samples.

1. Introduction

Metallic and non-metallic nanoparticles have broad applications in chemistry, physics, materials science, and industry. Among them, semiconductor metal oxides such as TiO_2, In_2O_3, CuO, NiO, and ZnO, along with their composites with carbon-based materials (carbon nanotubes, graphene, graphene oxide, and heterostructures), have attracted significant attention due to their technological importance [1]. These materials are widely investigated for gas-sensing applications because the adsorption of gas molecules on their surfaces induces measurable changes in electrical resistance [2]. Semiconductor metal oxide gas sensors are particularly appealing owing to their compact size, low cost, ease of fabrication, and high sensitivity to toxic and pollutant gases [3]. The sensing performance of these materials strongly depends on parameters such as grain size, crystallographic phase, microstructure, film thickness, additives, and intrinsic semiconductor properties. Careful control of these factors is essential to enhance sensitivity, selectivity, and stability [4]. Titanium dioxide (TiO_2) is one of the most extensively studied metal oxides for gas-sensing applications [5]. It is an n-type semiconductor with a wide band gap (~3 eV) and exhibits excellent chemical stability, environmental friendliness, and high-temperature resistance [6]. These properties make TiO_2 suitable not only for gas sensors but also for solar cells and photocatalytic applications [7]. TiO_2 exists in three crystalline phases: anatase, brookite (both metastable), and rutile (thermodynamically stable) [8]. Among them, anatase is most widely used for gas sensing due to its high concentration of oxygen vacancies and superior gas response [9]. However, anatase irreversibly transforms into rutile at temperatures between 600–800 °C, typically accompanied by grain growth, which can negatively affect sensing performance [10]. The phase transition temperature and grain growth behavior depend on preparation methods, precursors, and the presence of additives [11]. It has been reported that suitable additives can inhibit the anatase-to-rutile transformation and suppress grain growth, thereby improving thermal stability [12]. Hydrothermal treatment has emerged as an effective method to tailor the microstructure and enhance the thermal stability of semiconductor oxides [13]. Previous studies on materials such as SnO_2 have shown that hydrothermal processing improves structural stability and gas sensitivity [14]. Motivated by these findings, the present work investigates the influence of hydrothermal treatment on the structural, crystallographic, and electrical properties of TiO_2 [15]. After hydrothermal processing, the powders were calcined at temperatures between 600 and 900 °C, and thick films were fabricated to evaluate their ability to detect CO gas diluted in air [16]. At the nanoscale (1–100 nm), materials exhibit unique physical and chemical properties compared to their bulk counterparts, primarily due to their high surface-to-volume ratio [17]. Nanocrystalline semiconductor oxides therefore demonstrate enhanced optical, electrical, and catalytic properties [18].

As a result, significant research efforts have focused on the synthesis, characterization, and application of TiO_2 nanostructures and related nanocomposites. Overall, TiO_2 nanomaterials remain highly promising candidates for advanced gas-sensing applications due to their tunable structure, stability, and enhanced nanoscale properties.

*Corresponding Author:purvapatil2601@gmail.com(Purva B. Patil)

https://doi.org/10.30799/jnst.S203.26110303

2. Experimental Methods

2.1 Synthesis of Pure TiO_2

Titanium dioxide (TiO_2) nanoparticles were synthesized using a combined sol–gel and hydrothermal method, followed by calcination and thick-film fabrication for gas-sensing applications. Initially, a 0.5 M solution of titanium isopropoxide was prepared in isopropanol to prevent premature hydrolysis. This solution was added dropwise to aqueous nitric acid (HNO_3) under continuous stirring to achieve controlled hydrolysis and condensation. Two sols with pH values of 2 and 3 were prepared to examine the effect of acidity on structural evolution. The mixtures were peptized overnight to form stable titania sols, which gradually transformed into titanic acid gels. The gels were filtered, washed with deionized water, and dried at 120 °C. A portion of the dried gels was directly calcined at 600–900 °C for 3 hours to induce crystallization and phase transformation into anatase and rutile TiO_2. The remaining portion was redispersed in dilute HNO_3 (2 wt% TiO_2) and subjected to hydrothermal treatment at 150 °C for 3 hours in a Teflon-lined autoclave under mechanical stirring (500 rpm). The pH was maintained at 2 or 3, below the isoelectric point of TiO_2, to ensure electrostatic stabilization and prevent particle agglomeration. The resulting dispersions were dried at 120 °C and subsequently calcined at 600–900 °C to control crystallite size and phase composition. Structural characterization of the calcined powders was performed using X-ray diffraction (XRD) to determine crystal structure, phase composition, and average crystallite size. For sensor fabrication, the powders were mixed with ethylene glycol to form pastes and deposited onto alumina substrates with pre-patterned gold electrodes using the screen-printing technique.

3. Results and Discussion

3.1 UV–Visible Analysis

The UV–Visible spectrum of TiO_2 nanoparticles typically shows (Fig. 1) a strong and broad absorption band in the UV region, which is clearly reflected in the given graph where the absorbance begins around 1.5 Abs near 200–220 nm and gradually decreases with increasing wavelength. This high UV absorption arises from the intrinsic band-to-band electronic transition in TiO_2, specifically the O^{2-} (2p) → Ti^{4+} (3d) charge-transfer transition, which is characteristic of semiconductor metal oxides. As the wavelength progresses toward 350–400 nm, the absorbance starts to drop more steeply, indicating the absorption edge associated with the band gap of TiO_2 (typically ~3.2 eV for anatase and ~3.0 eV for rutile), and this edge often shifts slightly depending on nanoparticle size, crystallinity, and surface defects. Beyond approximately 450–500 nm, the spectrum flattens to near zero, showing that TiO_2 nanoparticles do not absorb in the visible region and thus remain optically transparent or white in appearance. The overall spectral pattern confirms the presence of nanoscale TiO_2 with strong UV-blocking capability, high excitonic absorption, and a clear band gap transition, making such nanoparticles useful in photocatalysis, UV-shielding coatings, and sunscreen formulations.

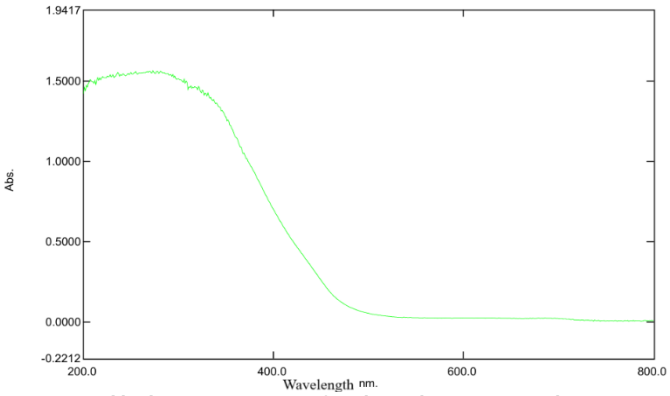

Fig. 1 UV–visible absorption spectrum of synthesized TiO_2 nanoparticles

3.2 FE-SEM Analysis

The FESEM micrographs of the TiO_2 nanoparticles reveal a predominantly quasi-spherical and irregularly aggregated morphology (Fig. 2), which is typical for metal-oxide nanoparticles synthesized through chemical or sol–gel routes. The particles appear densely packed, forming clusters and agglomerates due to their high surface energy and nanoscale dimensions. From the annotated size measurements visible in the images, the nanoparticles show an average size range of approximately 17–35 nm, indicating a uniform nanoscale distribution with only slight variation across different regions of the sample. The surface texture appears rough and granular, suggesting the presence of numerous small crystallites fused together, which is consistent with the formation of polycrystalline TiO_2. The high magnification images (200,000×) highlight clearly defined particle boundaries in several zones, while the lower magnification image (10,000×) displays the overall compact agglomerated structure across a wider area. This morphology supports the typical characteristics of TiO_2 nanoparticles that contribute to their enhanced photocatalytic activity, large surface area, and strong UV absorption capability.

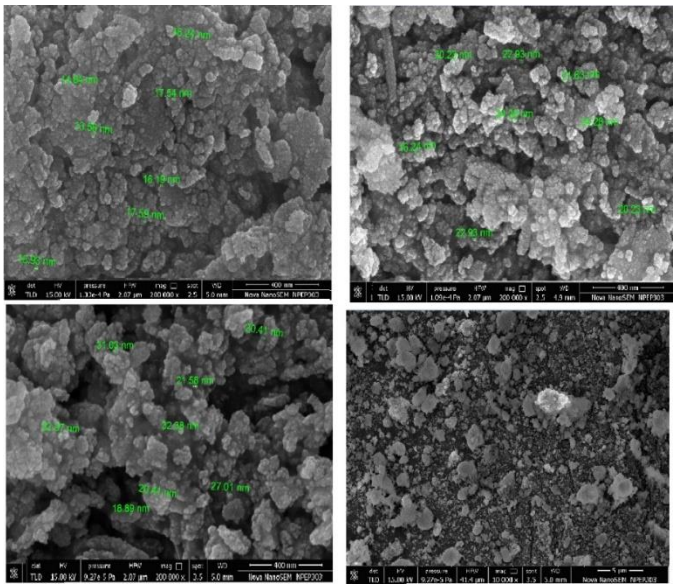

Fig. 2 SEM micrographs of synthesized TiO_2 nanoparticles

3.3 EDS Analysis

The EDS spectrum of the synthesized TiO_2 nanoparticles shows prominent and well-defined elemental peaks corresponding exclusively to titanium (Ti) and oxygen (O), confirming the successful formation and purity of the metal-oxide nanomaterial (Fig. 3). A strong Ti peak is observed around 4.5–5.0 keV, accompanied by additional characteristic Ti signals at lower energies, which are typical for Ti Kα and Kβ emission lines. The oxygen peak appears in the low-energy region near 0.5 keV, reflecting the presence of O Kα emissions, which are usually weaker but distinctly visible in oxide-based materials. The absence of any additional peaks related to impurities or unwanted elements indicates that the sample is chemically clean and free from contamination. The relative intensity of titanium compared to oxygen aligns with the expected stoichiometry of TiO_2, considering the limitations of EDS in quantitatively detecting light elements. Overall, the EDS profile strongly supports the formation of pure TiO_2 nanoparticles with no trace foreign elements, complementing the structural and morphological evidence obtained from FESEM analysis.

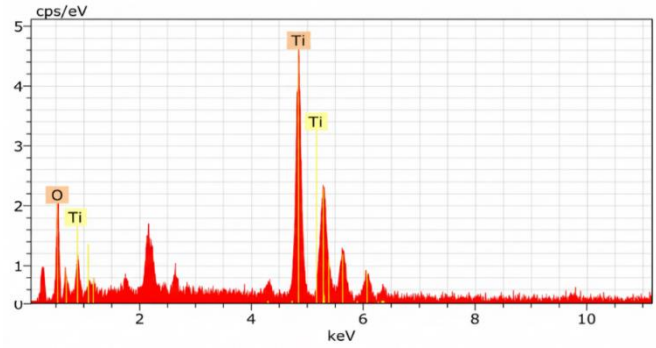

Fig. 3 EDX spectrum of synthesized TiO_2 nanocomposite

3.4 FT-IR Analysis

The FTIR spectrum of the synthesized TiO_2 nanoparticles exhibits several characteristic absorption bands that confirm the formation of metal–oxide structures along with surface-bound functional groups typically associated with nanoparticle synthesis (Fig. 4). The broad and intense band observed around 3423 cm^{-1} corresponds to the O–H stretching vibration of surface hydroxyl groups and adsorbed water

https://doi.org/10.30799/jnst.S203.26110303

molecules, a common feature in metal oxide nanoparticles due to their high surface area and hygroscopic nature. A weaker feature near 3857 cm^{-1} may also be attributed to isolated or free O–H stretching vibrations. The region around 1628 cm^{-1} represents the bending mode of molecular water (H–O–H), further indicating moisture adsorption on the nanoparticle surface. The peaks in the fingerprint region between 1350–900 cm^{-1} likely arise from residual organic moieties or precursor-related vibrations, which sometimes remain after synthesis, such as C–O or C–H bending modes. Most importantly, the strong and characteristic absorption bands below 700 cm^{-1}, especially those observed near 689, 619, 556, and 525 cm^{-1}, correspond to the Ti–O and Ti–O–Ti stretching vibrations, which are definitive markers of TiO_2 lattice formation. The presence of these low-wavenumber metal–oxygen vibrational peaks confirm the successful synthesis of TiO_2 nanoparticles, while the O–H and water-related bands indicate typical surface functionality that can influence photocatalytic and adsorption properties.

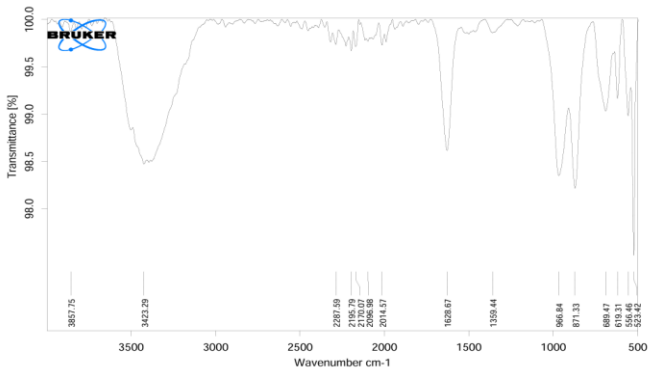

Fig. 4 FTIR spectrum of synthesized TiO_2 nanocomposite

3.5 XRD Analysis

The XRD pattern of the synthesized TiO_2 nanoparticles shows a series of sharp, intense diffraction peaks between 20° and 70° (2θ), indicating a well-crystallized structure with clearly resolved lattice planes (Fig. 5). The most prominent peak appears near 25–27°, which corresponds to the (101) plane characteristic of the anatase phase of TiO_2, suggesting that anatase is the dominant crystalline form in the sample. Additional peaks observed around 37°, 48°, 54°, 55°, 62°, and 68° can be indexed to the (004), (200), (105), (211), (204), and (220) planes, respectively, further confirming the anatase crystal structure as reported in standard JCPDS data (JCPDS card no. 21-1272). The narrow and well-defined peaks indicate high crystallinity and small crystalline domains, typical of TiO_2 nanoparticles. The absence of major rutile or brookite peaks suggests that the synthesis method successfully produced phase-pure anatase TiO_2. The peak broadening at lower intensities also implies nanoscale crystallite size, consistent with FESEM-derived particle dimensions. Overall, the XRD profile confirms the formation of highly crystalline, phase-pure anatase TiO_2 nanoparticles with well-defined structural order.

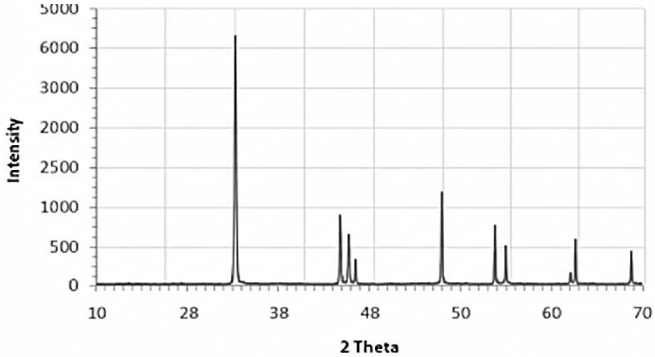

Fig. 5 X-ray diffraction (XRD) pattern of synthesized TiO_2 nanocomposite

3.6 Gas Sensing Results

The first graph shows how the gas-sensing performance of TiO_2 nanoparticles varies with temperature for ethanol, LPG, methanol, and CO_2 (Fig. 6). All gases exhibit a similar trend in which sensitivity increases from 40 °C to an optimal point at 120 °C, followed by a rapid decline at higher temperatures. Ethanol displays the strongest interaction with TiO_2, rising sharply to a peak sensitivity of ~65% at 120 °C, indicating highly efficient surface reaction kinetics at this temperature. LPG and methanol present moderate sensitivities (~24% and ~17%, respectively), while CO_2 remains consistently low, suggesting weak adsorption or limited surface reactivity. The drop in response after 120 °C is attributed to dominant desorption at elevated temperatures, where gas molecules cannot remain attached to the sensor surface long enough to produce significant resistance changes. Overall, the results confirm that the optimal operating temperature for TiO_2 gas sensing is around 120 °C, and TiO_2 shows the highest affinity toward ethanol, followed by LPG, methanol, and CO_2.

The second graph illustrates the dynamic sensing behavior of the TiO_2 sensor over two complete ON–OFF cycles, showing how quickly the material responds to and recovers from gas exposure. During each ON period, the sensitivity rises rapidly from 0 to ~65% within about 60 seconds, demonstrating fast adsorption and reaction of gas molecules with the TiO_2 surface. When the gas is removed, the sensor exhibits a smooth and consistent decline back to near-zero sensitivity in approximately 40 seconds, indicating effective desorption and strong surface regeneration capability. The nearly identical peak heights and repeating cycle patterns reflect excellent reproducibility and stability, which are crucial for real-time sensing applications. Overall, the dynamic response curve highlights the sensor's fast response, rapid recovery, and high repeatability, confirming the suitability of TiO_2 nanoparticles for reliable and continuous gas detection.

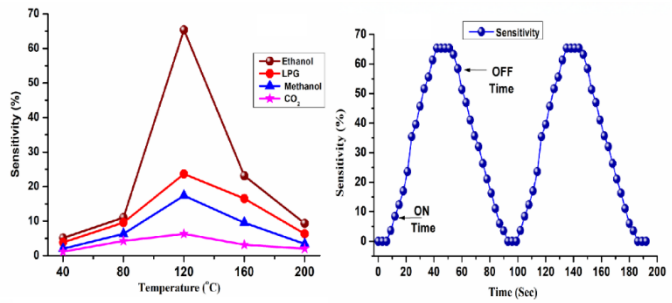

Fig. 6 (a) Gas sensing performance of TiO_2 nanoparticles showing (i) sensitivity (%) toward ethanol, LPG, methanol. (ii) CO_2 as a function of operating temperature (40–200 °C) and (b) dynamic response–recovery characteristics (ON/OFF cycles) of sensitivity versus time

4. Conclusion

Hydrothermal synthesis proved highly effective for producing thermally stable TiO_2 nanocrystals with a dominant anatase phase and controlled nanoscale morphology. Treatment at pH 3 significantly enhanced resistance to grain growth and anatase-to-rutile transformation, maintaining anatase crystallinity even at 800 °C, whereas untreated samples fully converted to rutile. The stabilized nanostructure exhibited crystallite sizes of ~13 nm at 600 °C and ~34 nm at 800 °C, confirming improved thermal durability. Comprehensive characterization by XRD, FESEM, UV–Vis, FTIR, and EDS verified high crystallinity, chemical purity, strong UV absorption, and uniform quasi-spherical morphology. The synthesized TiO_2 nanoparticles demonstrated excellent gas-sensing performance, with maximum sensitivity at an optimal operating temperature of 120 °C. Enhanced sensing behavior characterized by rapid response (~60 s), quick recovery (~40 s), and stable repeatability—was attributed to the high surface area, small grain size, and abundant active sites of the stabilized anatase phase. Sensitivity followed the trend, ethanol > LPG > methanol > CO_2, highlighting strong affinity toward volatile organic compounds. Overall, controlled hydrothermal treatment effectively tailors the structural and functional properties of TiO_2 nanomaterials, resulting in improved thermal stability, surface reactivity, and sensing efficiency. These findings confirm the strong potential of anatase TiO_2 nanoparticles for environmental monitoring and advanced semiconductor gas sensor applications.

References

[1] A.S. Morshedy, E.M. El-Fawal, E. Amdeha, Photocatalytic applications of metal oxide nanoparticles, in: Metal oxides, CRC Press, USA, 2025, pp.95–118.
[2] S. Yang, C. Jiang, S. Wei, Gas sensing in 2D materials, Appl. Phys. Rev. 4 (2017) 011103.
[3] N.K. Chowdhury, B. Bhowmik, Micro/nanostructured gas sensors: the physics behind the nanostructure growth, sensing and selectivity mechanisms, Nanoscale Adv. 3 (2021) 73–93.
[4] J.M. Rzaij, A.M. Abass, Review on TiO_2 thin film as a metal oxide gas sensor, J. Chem. Mater. Res. 2 (2020) 114–121.
[5] A.J. Albarakati, I.A. Matter, N-type metal oxide semiconductor: materials and their environmental applications, Biointerface Res. Appl. Chem. 13 (2023) 519.

https://doi.org/10.30799/jnst.S203.26110303

[6] J. Bai, B. Zhou, Titanium dioxide nanomaterials for sensor applications, Chem. Rev. 114 (2014) 10131–10176.
[7] D. Reyes-Coronado, G. Rodríguez-Gattorno, M.E. Espinosa-Pesqueira, C. Cab, R. de Coss, et al., Phase-pure TiO_2 nanoparticles: anatase, brookite and rutile, Nanotechnology 19 (2008) 145605.
[8] H. Tang, K. Prasad, R. Sanjinés, F. Lévy, TiO_2 anatase thin films as gas sensors, Sens. Actuators B Chem. 26 (1995) 71–75.
[9] K. Zakrzewska, M. Radecka, TiO_2-based nanomaterials for gas sensing: influence of anatase and rutile contributions, Nanoscale Res. Lett. 12 (2017) 89.
[10] S.G. Kumar, K.S.R. Rao, Polymorphic phase transition among the titania crystal structures using a solution-based approach: from precursor chemistry to nucleation process, Nanoscale 6 (2014) 11574–11632.
[11] D.A.H. Hanaor, C.C. Sorrell, Review of the anatase to rutile phase transformation, J. Mater. Sci. 46 (2011) 855–874.
[12] W. Shi, S. Song, H. Zhang, Hydrothermal synthetic strategies of inorganic semiconducting nanostructures, Chem. Soc. Rev. 42 (2013) 5714–5743.
[13] A.S. Jasim, O.N. Salman, The effect of solvent variation on structural, optical, and electrical properties of TiO_2 films prepared by hydrothermal method, J. Appl. Sci. Nanotechnol. 3 (2023) 59–69.
[14] A.M. Ruiz, G. Sakai, A. Cornet, K. Shimanoe, Microstructure control of thermally stable TiO_2 obtained by hydrothermal process for gas sensors, Sens. Actuators B Chem. 103 (2004) 312–317.
[15] J. Biener, A. Wittstock, T.F. Baumann, J. Weissmüller, M. Bäumer, et al., Surface chemistry in nanoscale materials, Materials 2 (2009) 2404–2428.
[16] M.H. Huang, G. Naresh, H.S. Chen, Facet-dependent electrical, photocatalytic, and optical properties of semiconductor crystals and their implications for applications, ACS Appl. Mater. Interfaces 10 (2018) 4–15.
[17] J. Prakash, P. Kumar, R.A. Harris, C. Swart, J.H. Neethling, et al., Synthesis, characterization and multifunctional properties of plasmonic Ag–TiO_2 nanocomposites, Nanotechnology 27 (2016) 355707.
[18] Y. Wang, T. Wu, Y. Zhou, C. Meng, W. Zhu, L. Liu, TiO_2-based nanoheterostructures for promoting gas sensitivity performance: designs, developments, and prospects, Sensors 17 (2017) 1971.

https://doi.org/10.30799/jnst.S203.26110303

Cite this Article as: Purva B. Patil, Gokul V. Suryawanshi, Tulshidas S. Savale, Synthesis and characterization of TiO_2 nanoparticles for gas sensing applications, J. Nanosci. Tech. 11(3) (2026) 1086–1089.